Supporting Information

Mixed-conducting property of annealed polyacrylonitrile activated by n-doping of conjugated domains

M. C. Schulze[a] and A. L. Prieto[a]

[a] *Department of Chemistry, Colorado State University, Fort Collins, Colorado 80523, United States*

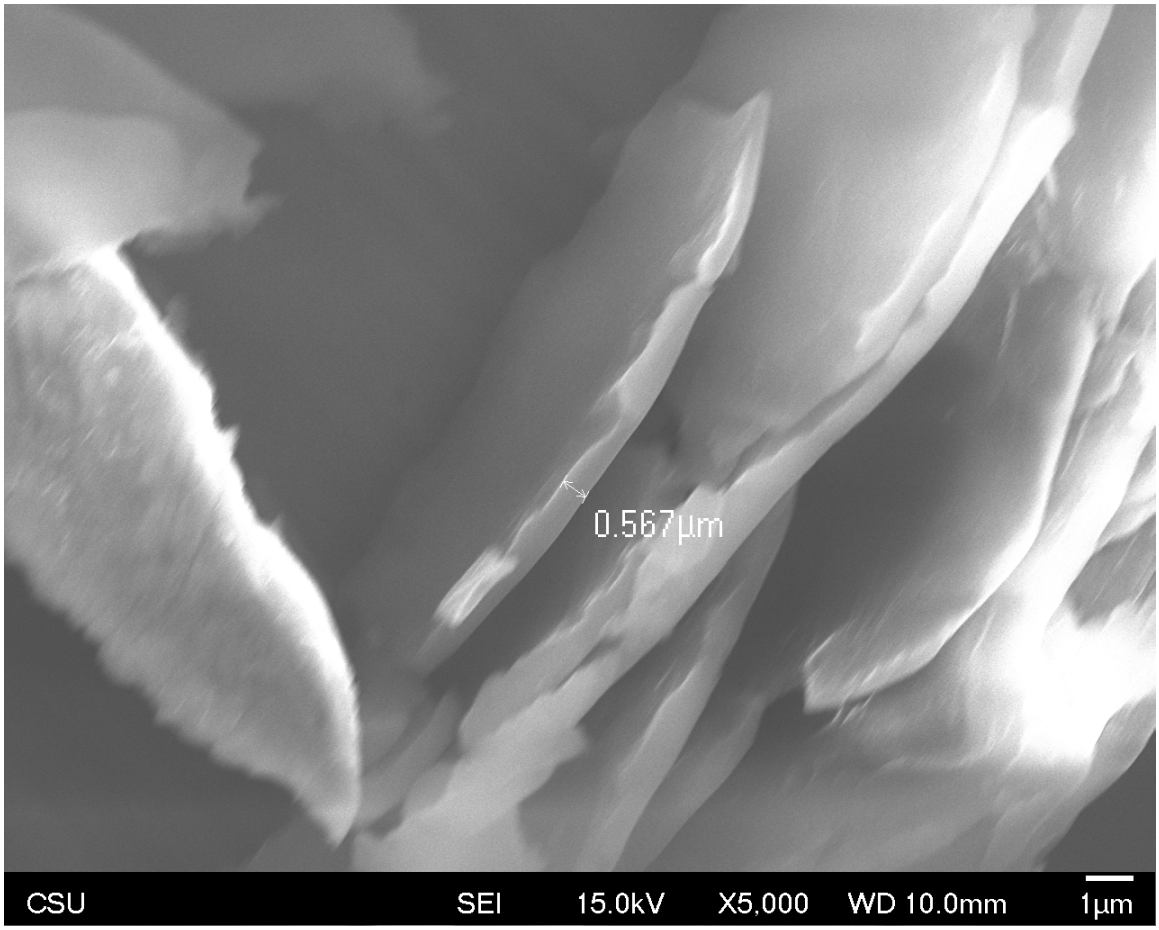

Figure S1. An SEM image of an annealed PAN film that was purposely damaged to expose an edge of the film to be measured. The thicknesses of the films prepared this way were measured around 0.5 um thick.

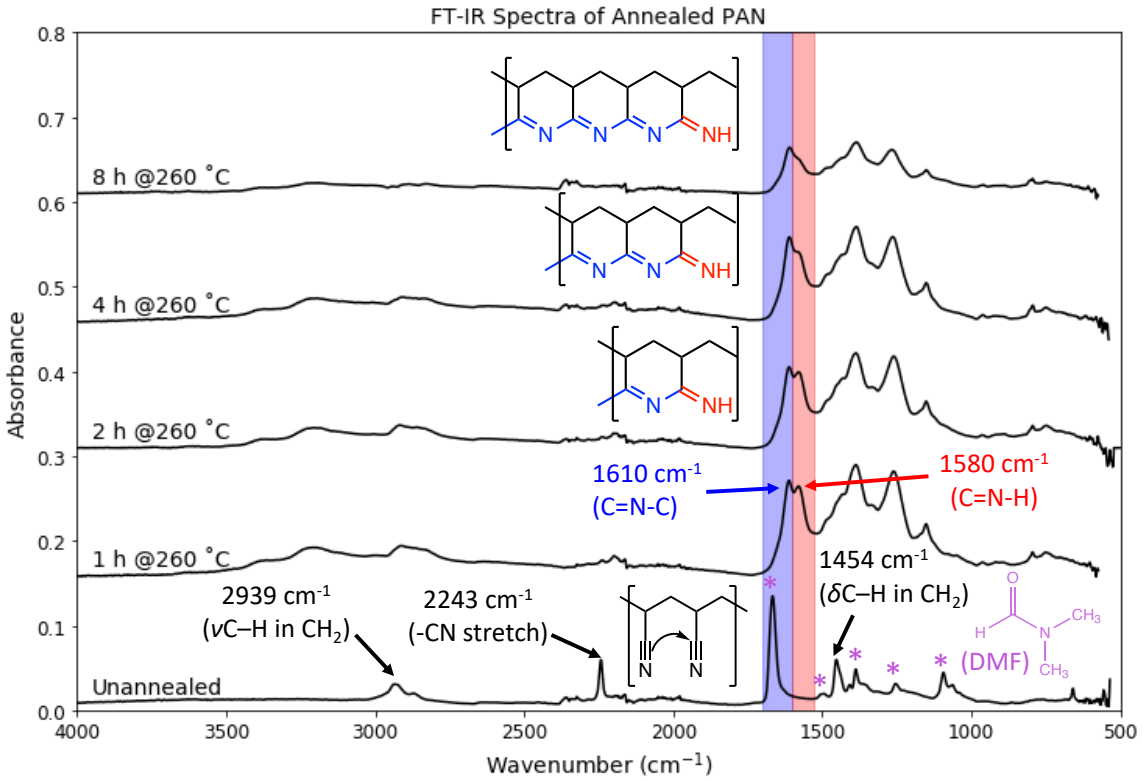

Figure S2. Representative FT-IR spectra of annealed PAN films. Critical features in the IR spectra are marked or highlighted and correlate to the structural features indicated in the inlayed structures.

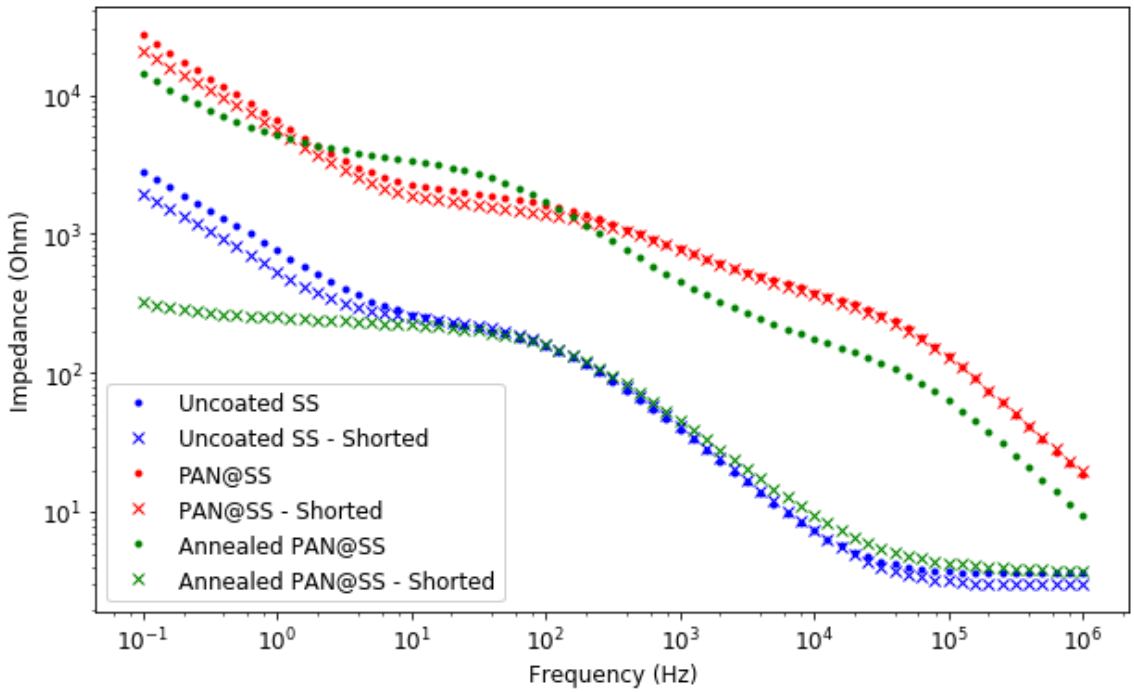

Figure S3. Several representative EIS spectra of annealed PAN electrodes in Li-ion half-cells. The annealed PAN@SS electrode was annealed at 300˚C for 3 hours so it is sufficiently conjugated to be electrically conducting when n-doped (shorted).

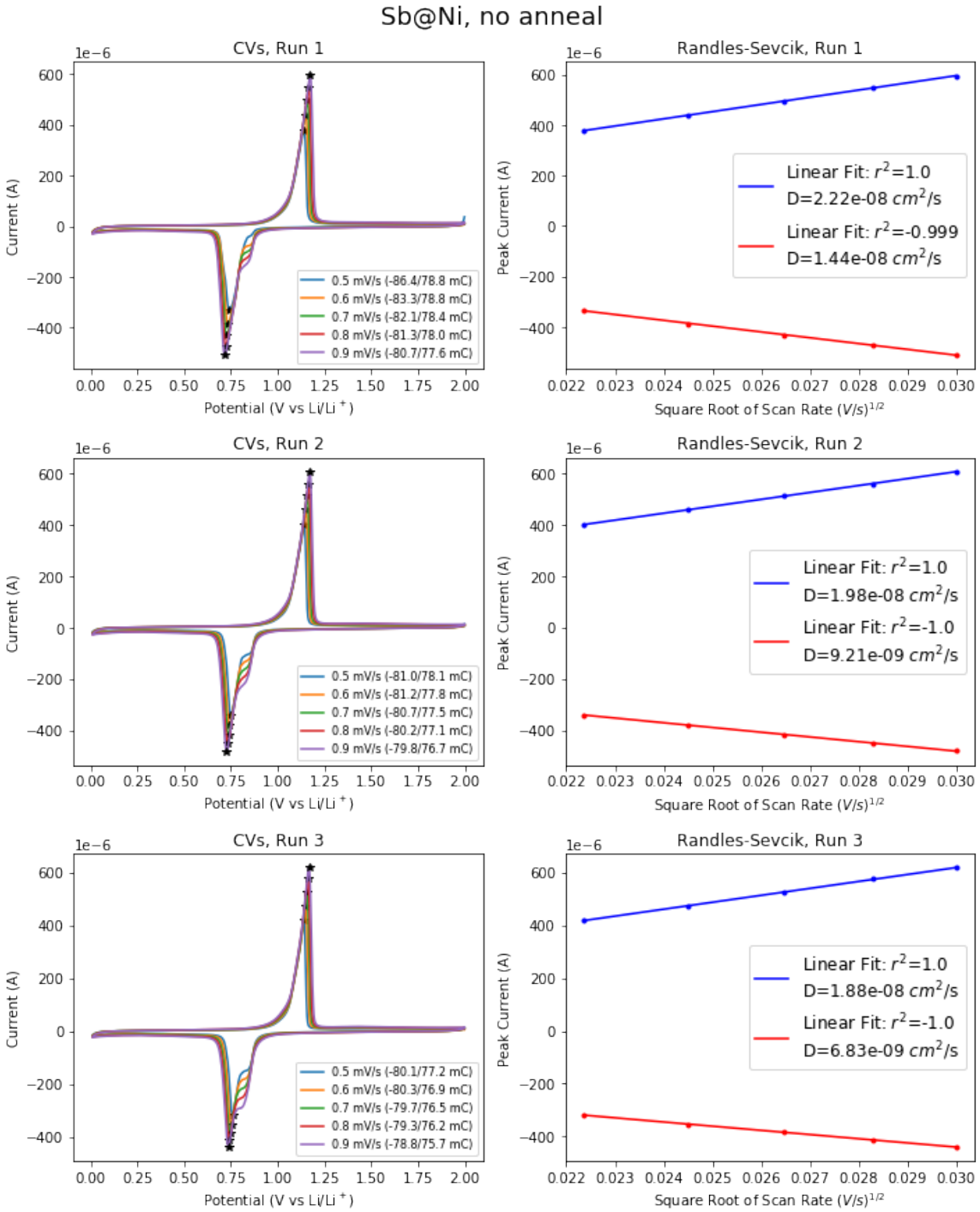

Figure S4. Variable rate CVs of the uncoated and unannealed Sb@Ni electrode with the corresponding bottleneck diffusivities calculated using the Randles-Sevcik equation.

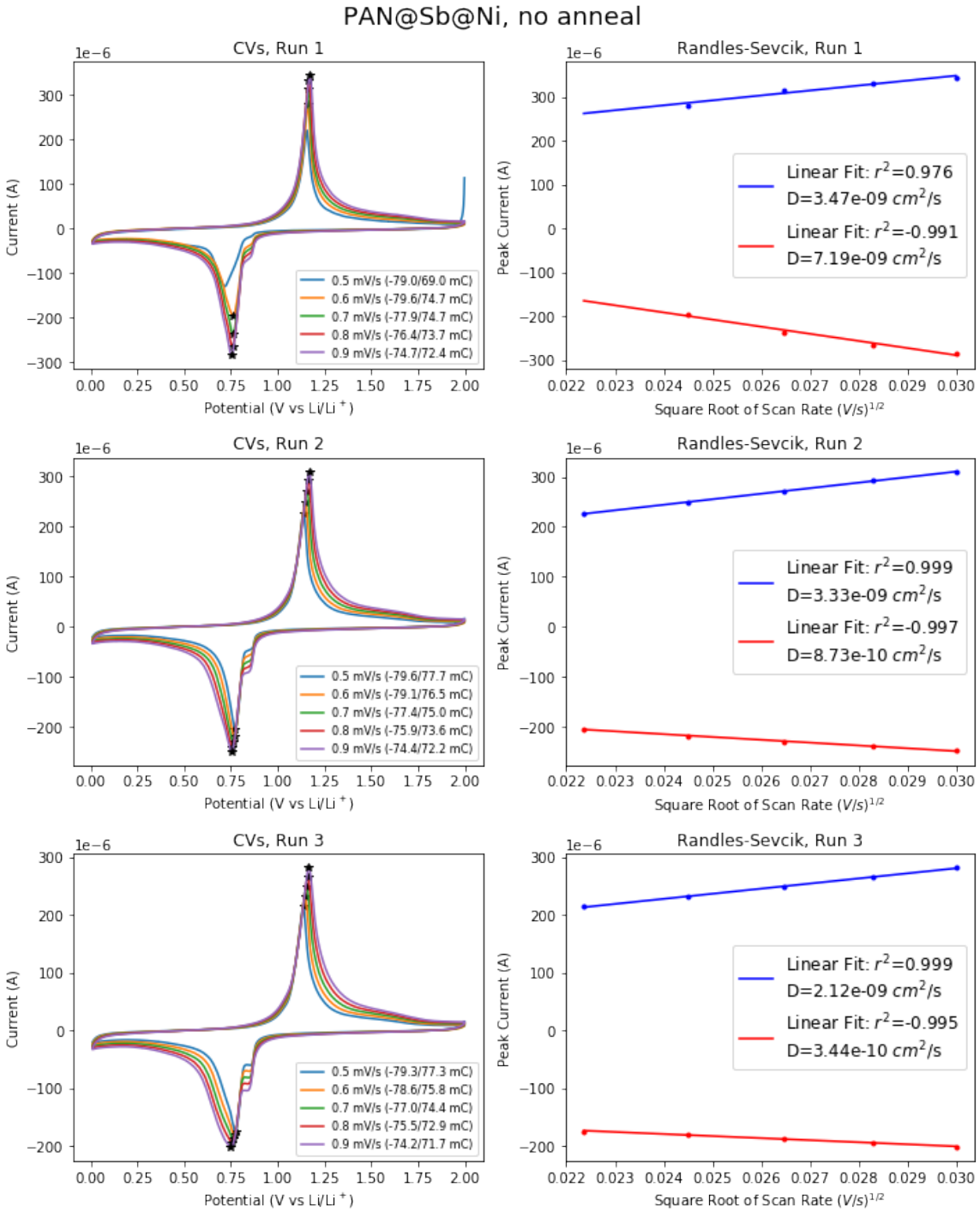

Figure S5. Variable rate CVs of the unannealed PAN@Sb@Ni electrode with the corresponding bottleneck diffusivities calculated using the Randles-Sevcik equation.

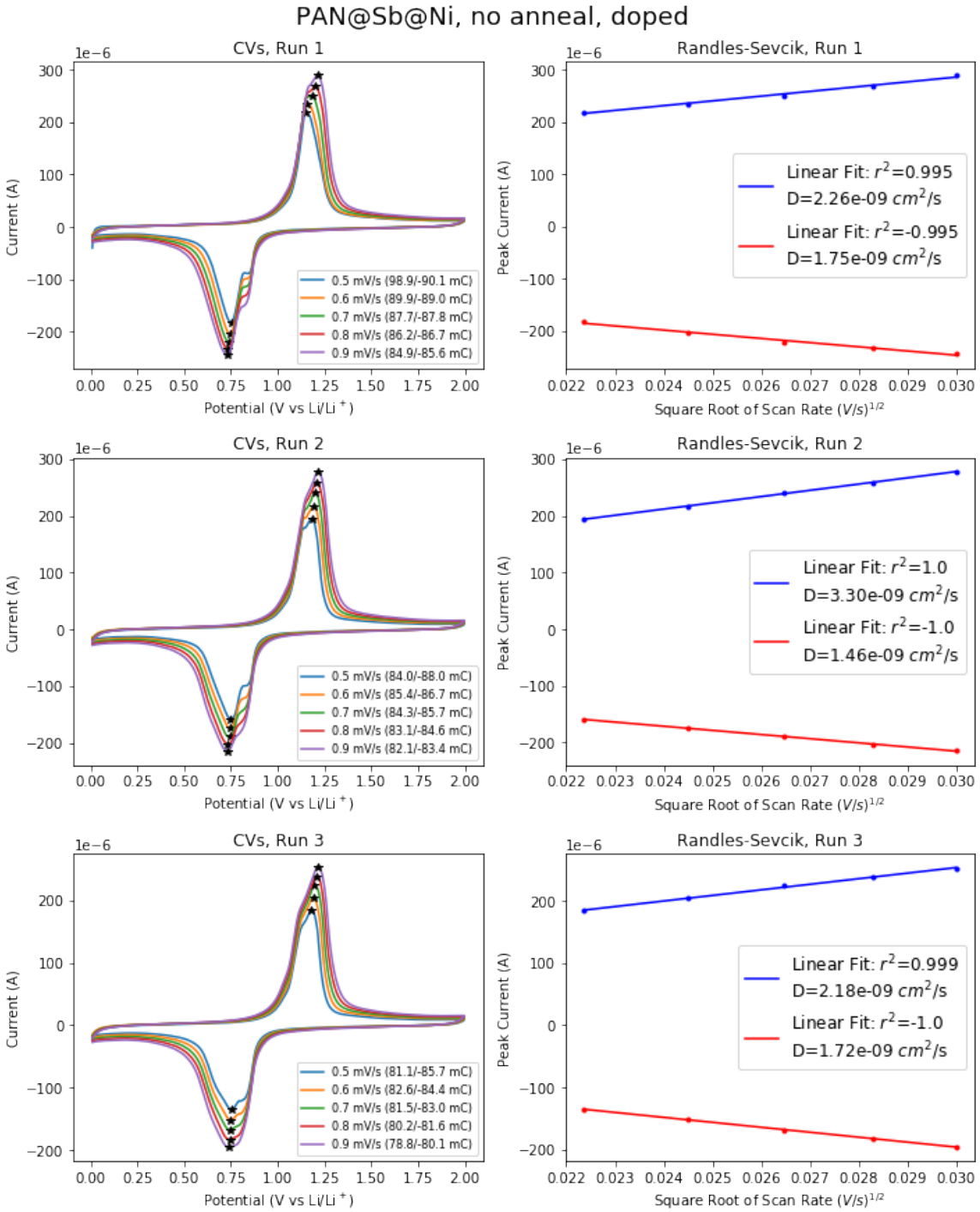

Figure S6. Variable rate CVs of the unannealed and doped (shorted) PAN@Sb@Ni electrode with the corresponding bottleneck diffusivities calculated using the Randles-Sevcik equation.

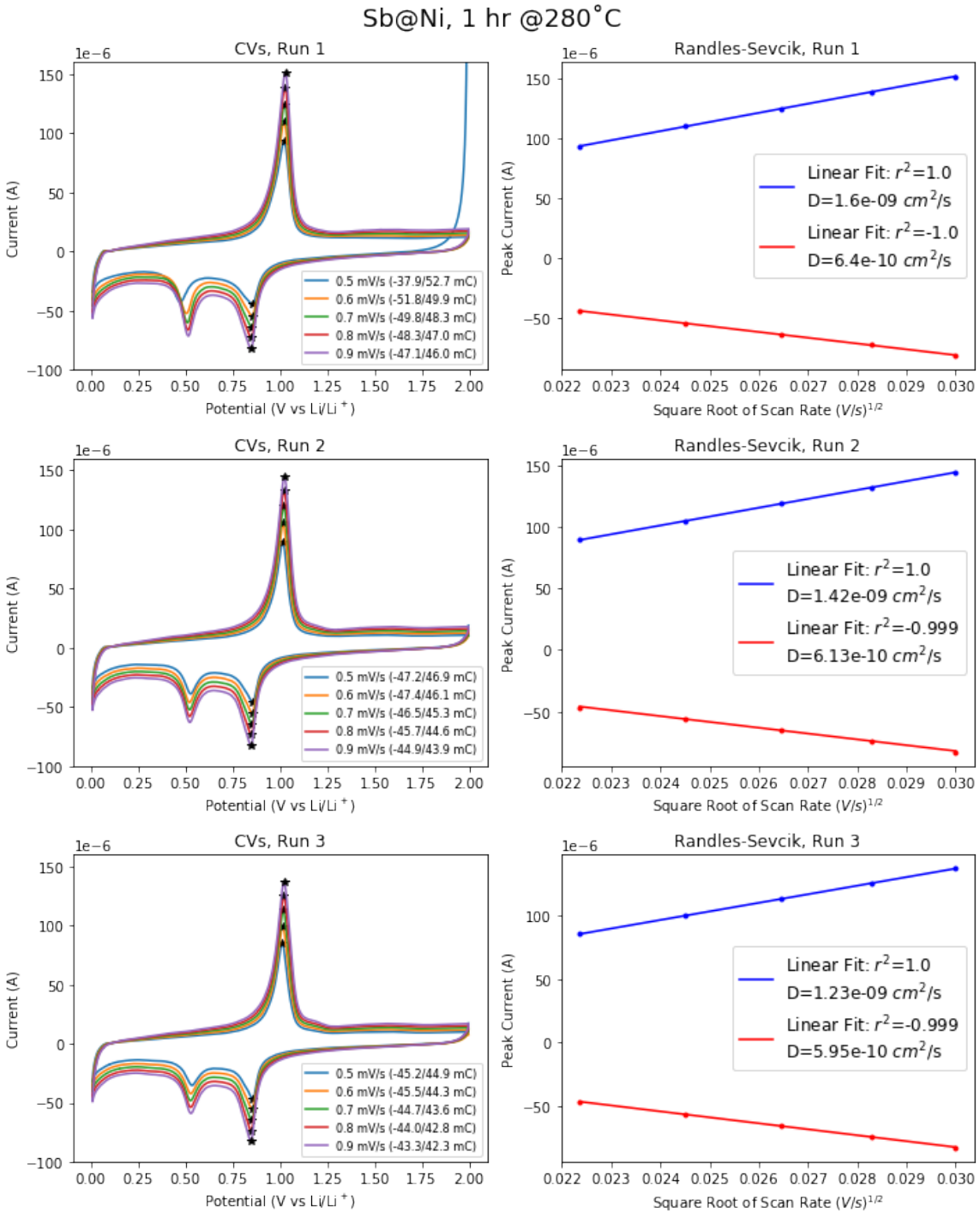

Figure S7. Variable rate CVs of the uncoated and 1 hour annealed Sb@Ni electrode with the corresponding bottleneck diffusivities calculated using the Randles-Sevcik equation.

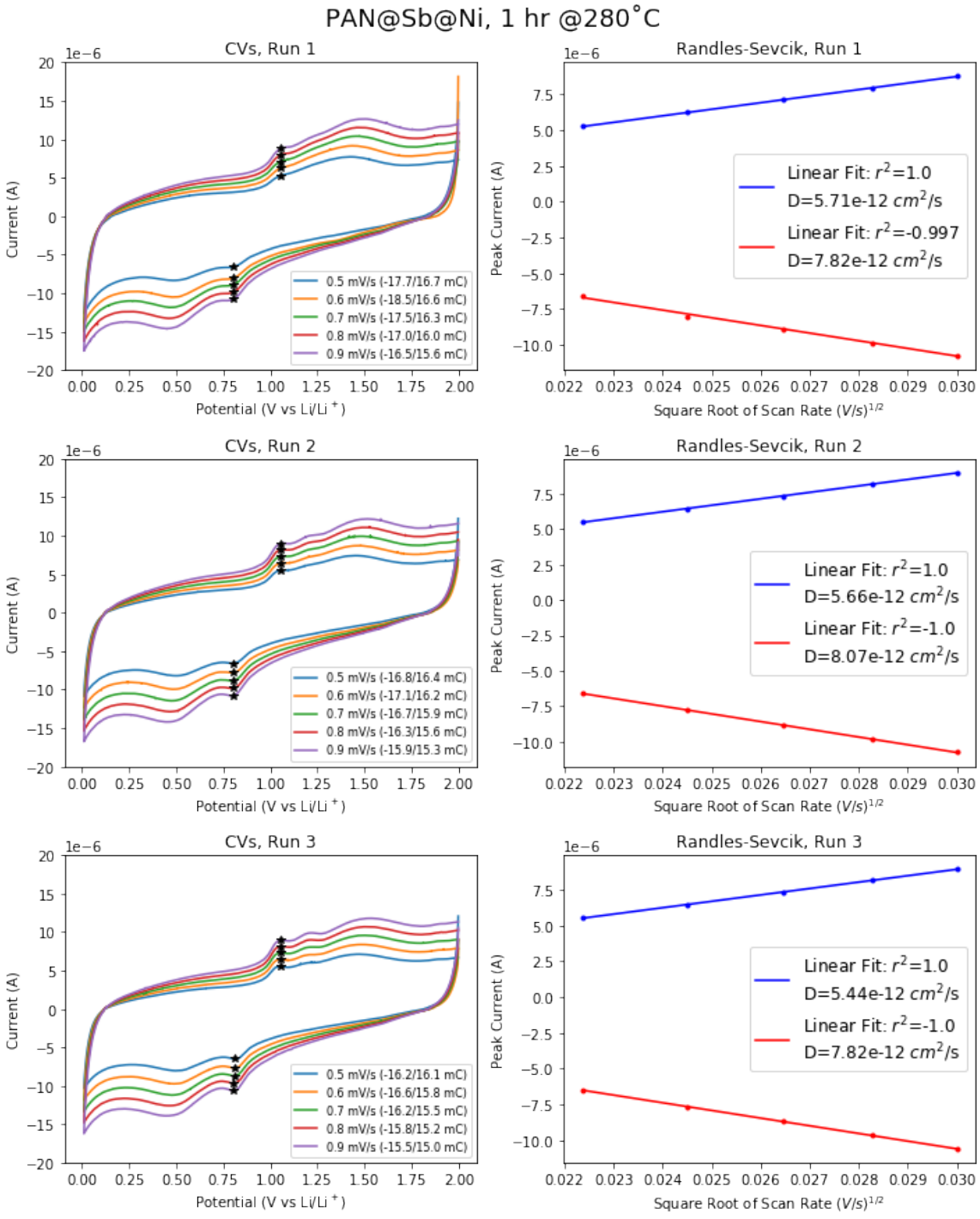

Figure S8. Variable rate CVs of the 1 hour annealed PAN@Sb@Ni electrode with the corresponding bottleneck diffusivities calculated using the Randles-Sevcik equation.

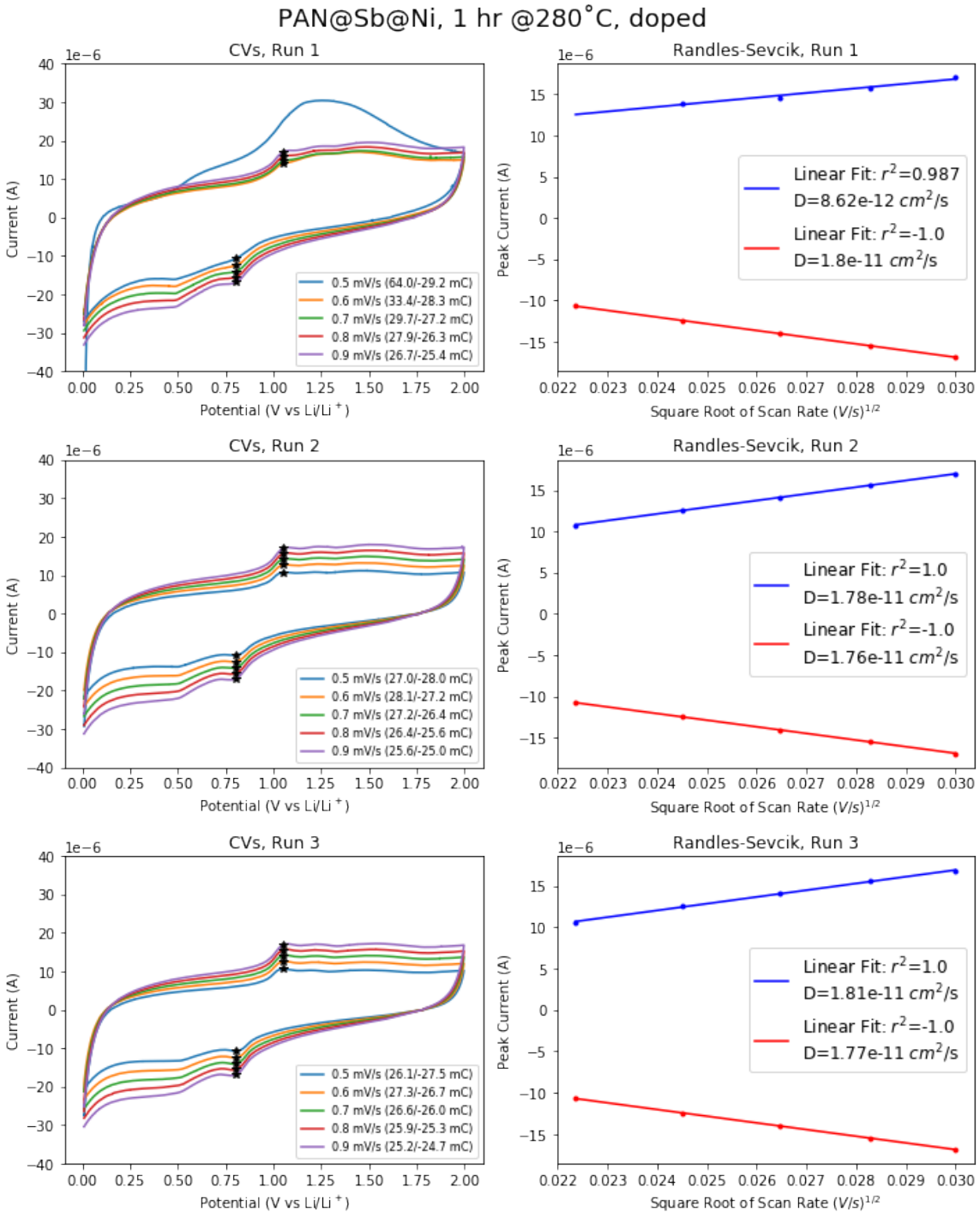

Figure S9. Variable rate CVs of the 1 hour annealed and doped (shorted) PAN@Sb@Ni electrode with the corresponding bottleneck diffusivities calculated using the Randles-Sevcik equation.

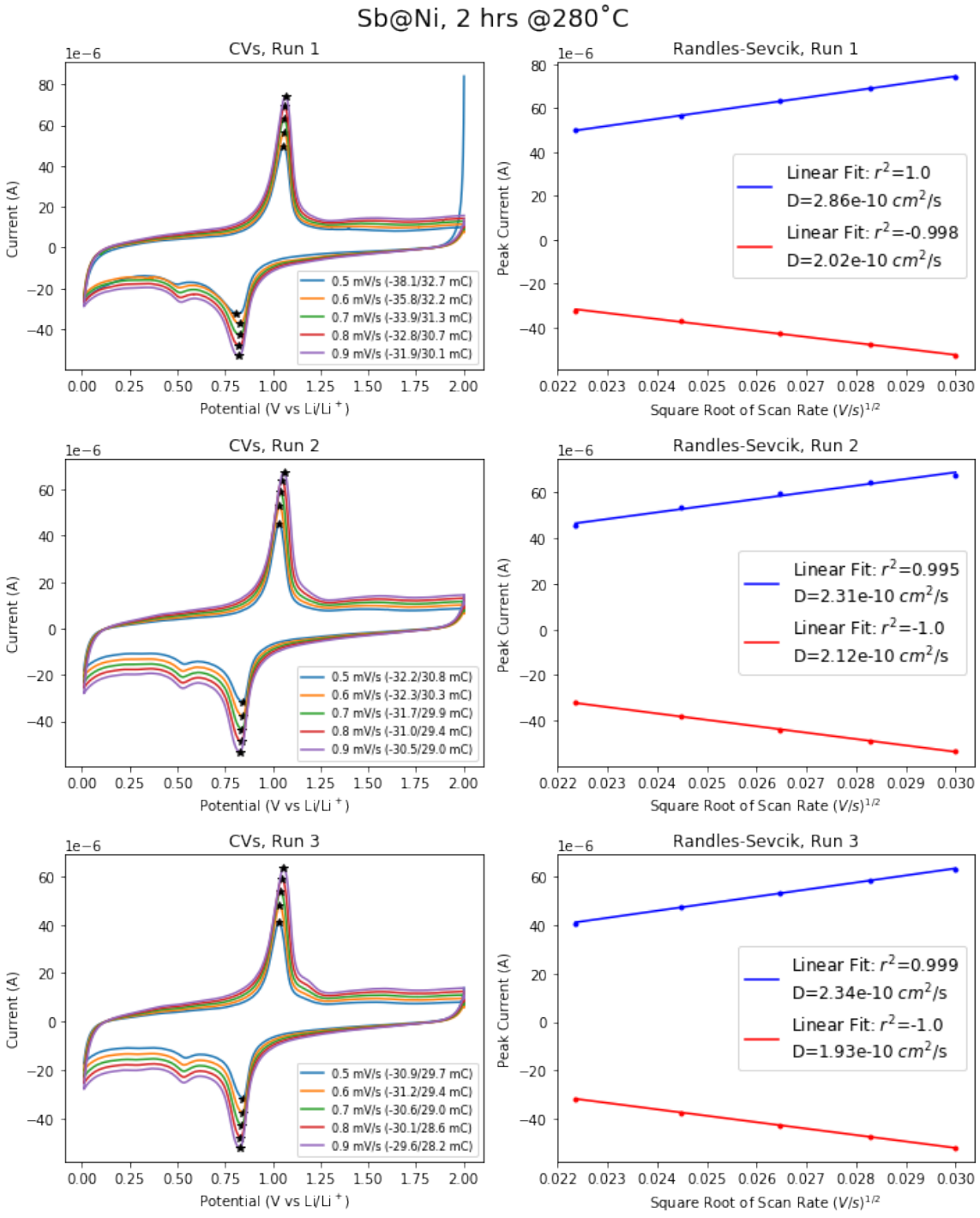

Figure S10. Variable rate CVs of the uncoated and 2 hour annealed Sb@Ni electrode with the corresponding bottleneck diffusivities calculated using the Randles-Sevcik equation.

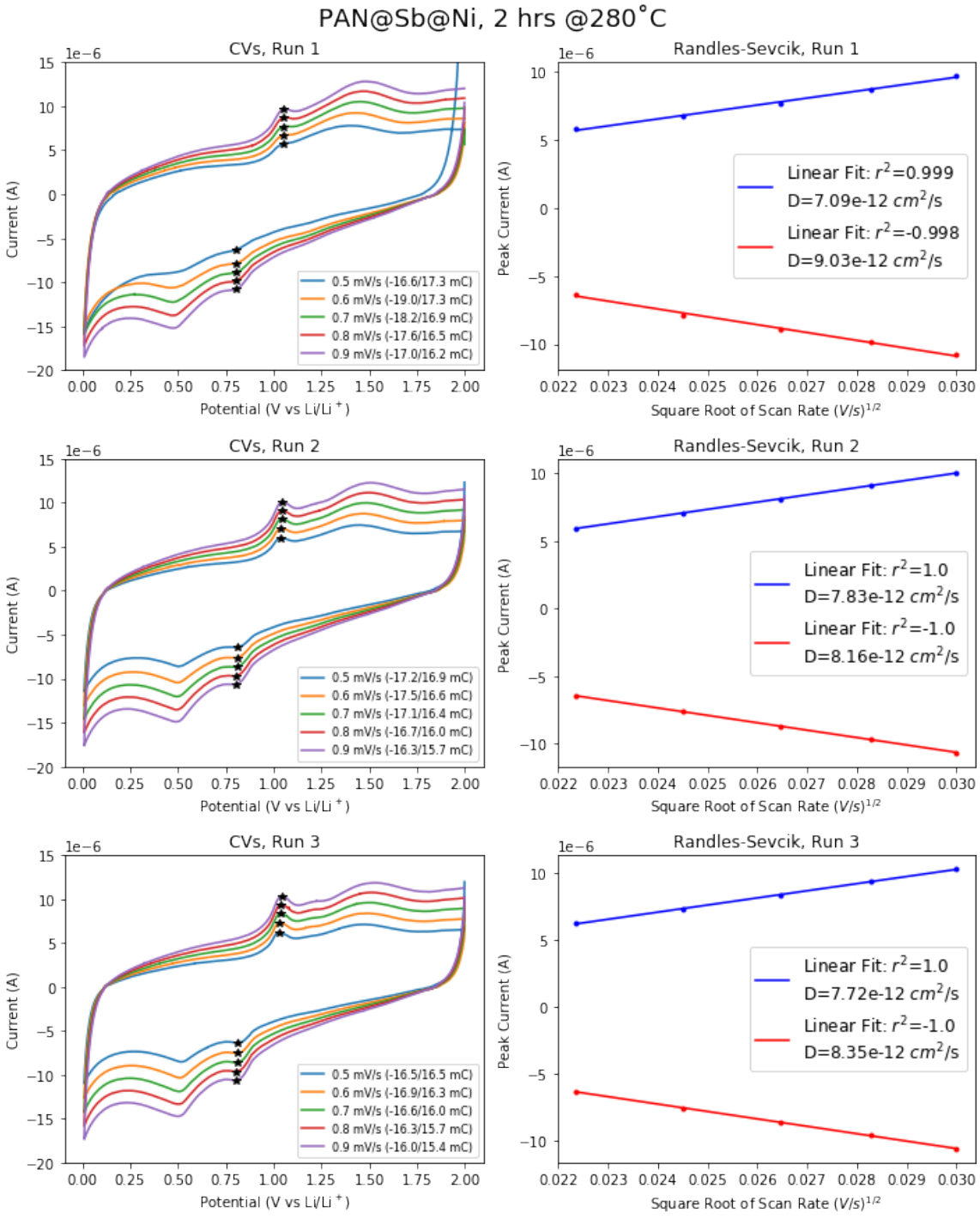

Figure S11. Variable rate CVs of the 2 hour annealed PAN@Sb@Ni electrode with the corresponding bottleneck diffusivities calculated using the Randles-Sevcik equation.

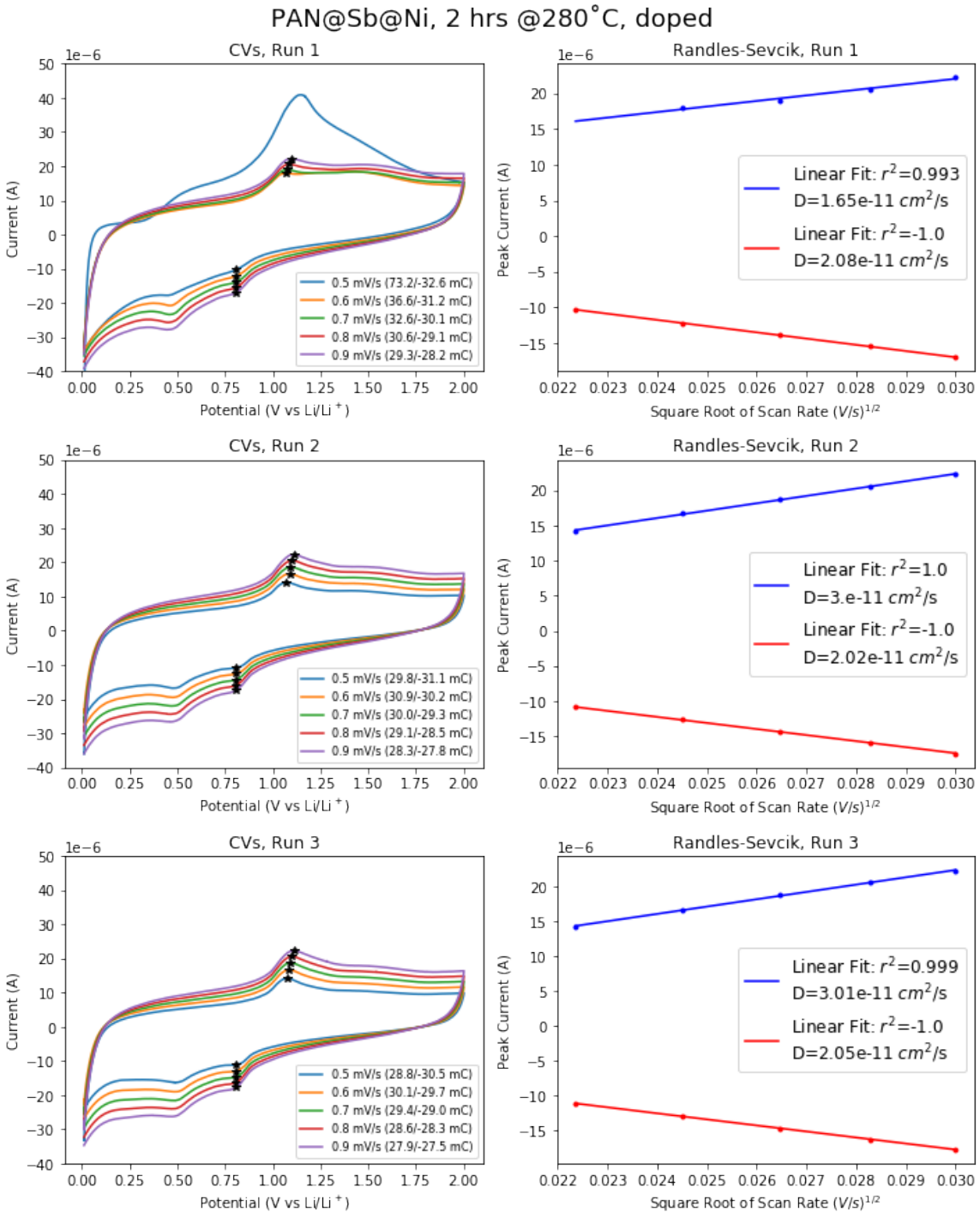

Figure S12. Variable rate CVs of the 2 hour annealed and doped (shorted) PAN@Sb@Ni electrode with the corresponding bottleneck diffusivities calculated using the Randles-Sevcik equation.

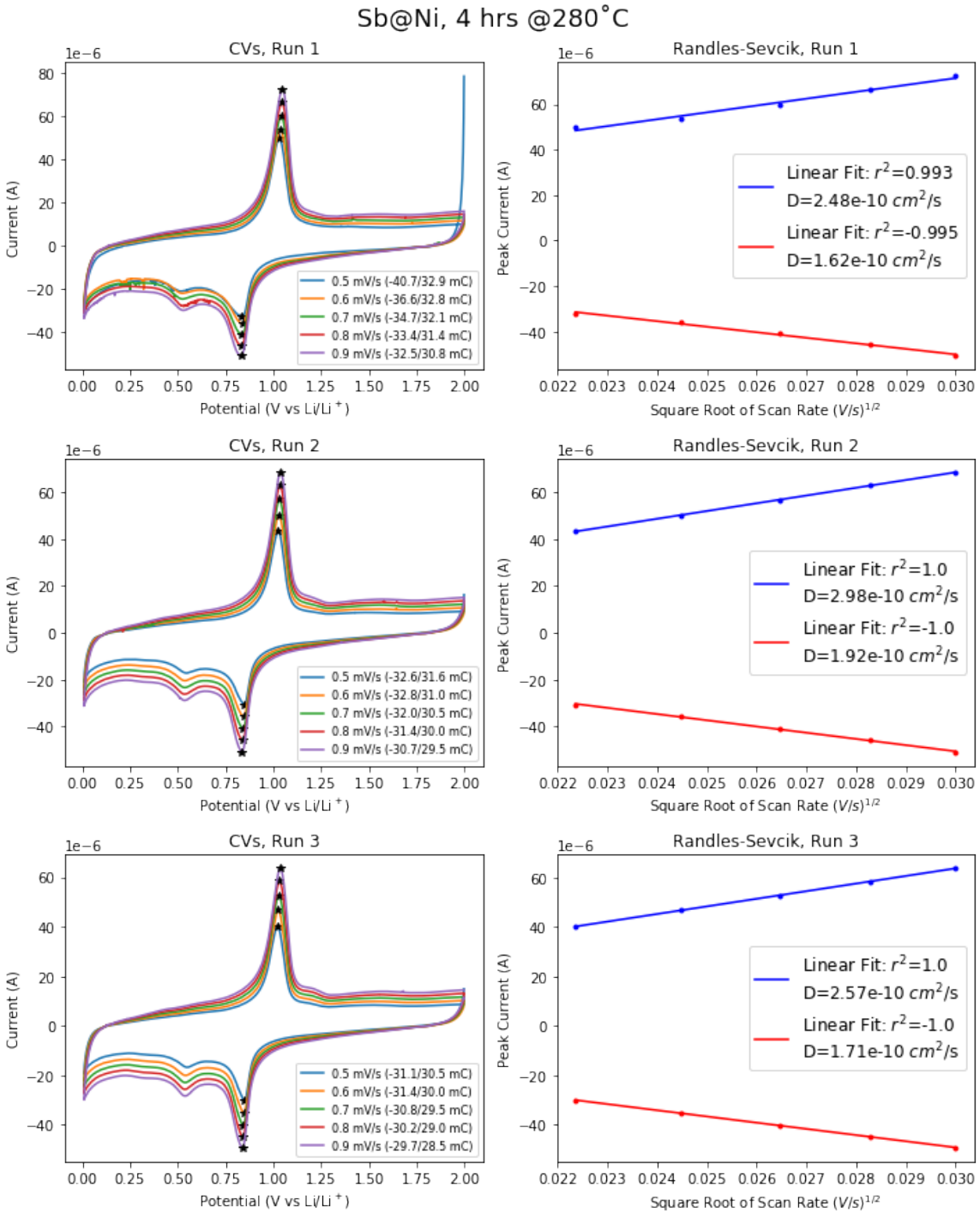

Figure S13. Variable rate CVs of the uncoated and 4 hour annealed Sb@Ni electrode with the corresponding bottleneck diffusivities calculated using the Randles-Sevcik equation.

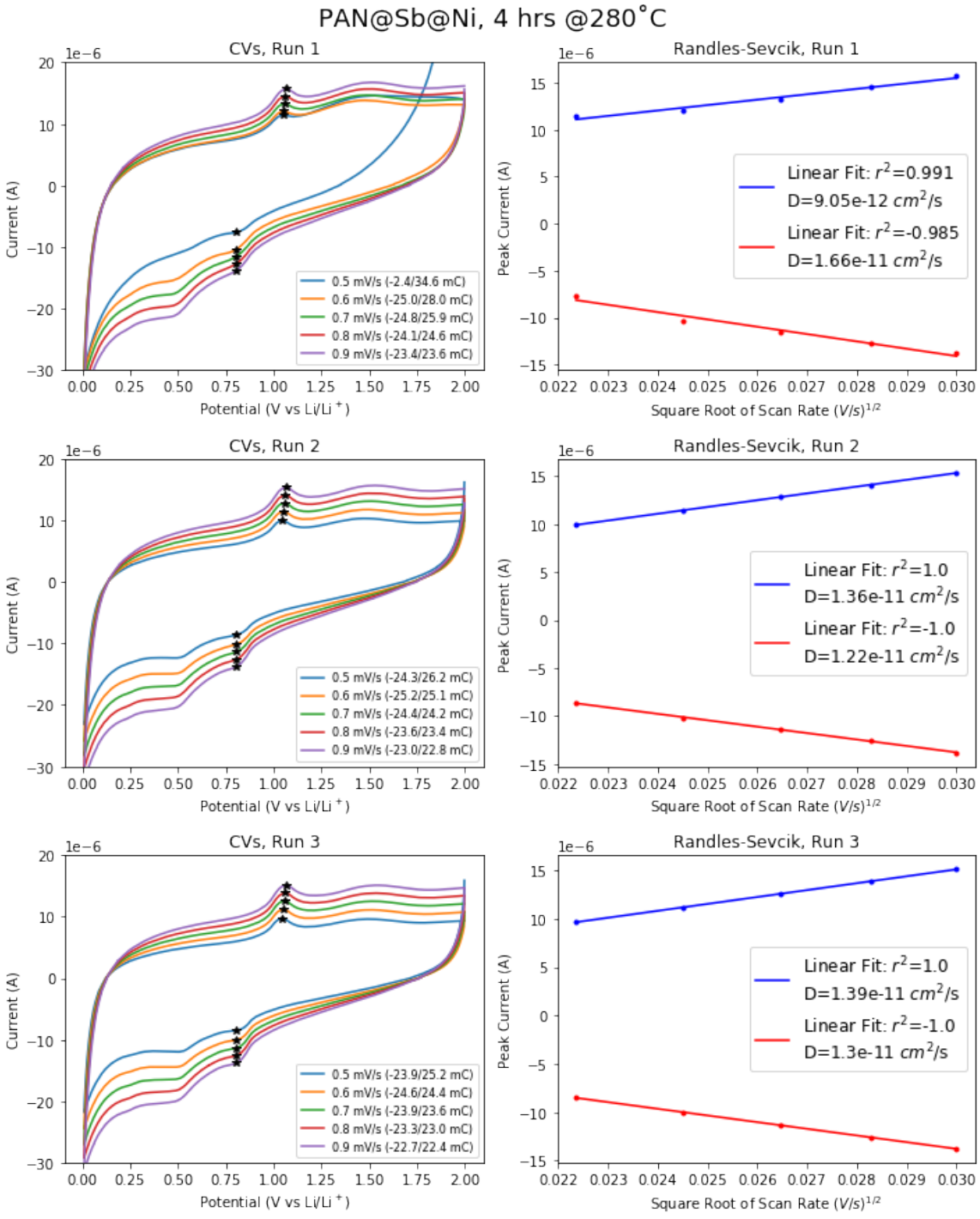

Figure S14. Variable rate CVs of the 4 hour annealed PAN@Sb@Ni electrode with the corresponding bottleneck diffusivities calculated using the Randles-Sevcik equation.

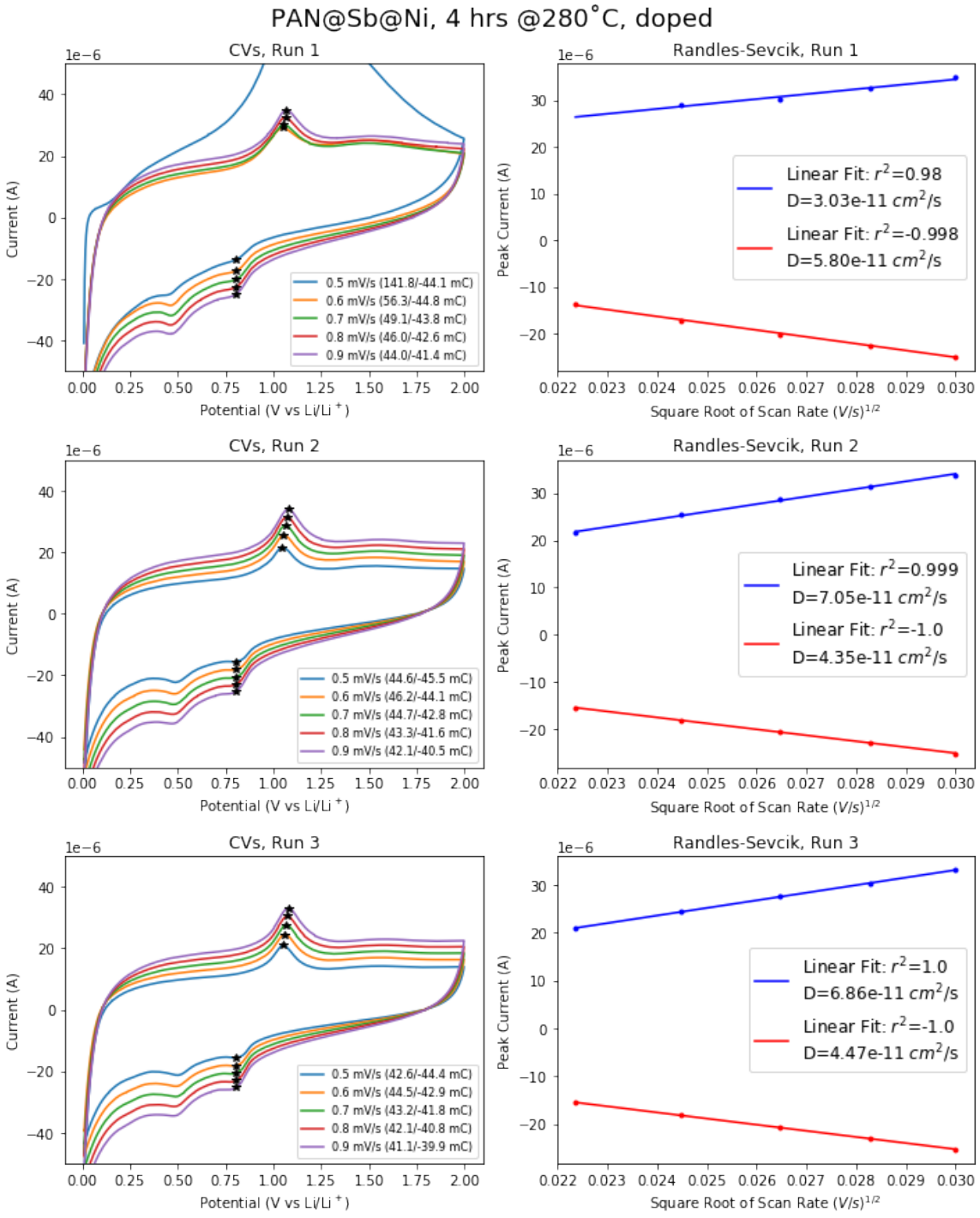

Figure S15. Variable rate CVs of the 4 hour annealed and doped (shorted) PAN@Sb@Ni electrode with the corresponding bottleneck diffusivities calculated using the Randles-Sevcik equation.

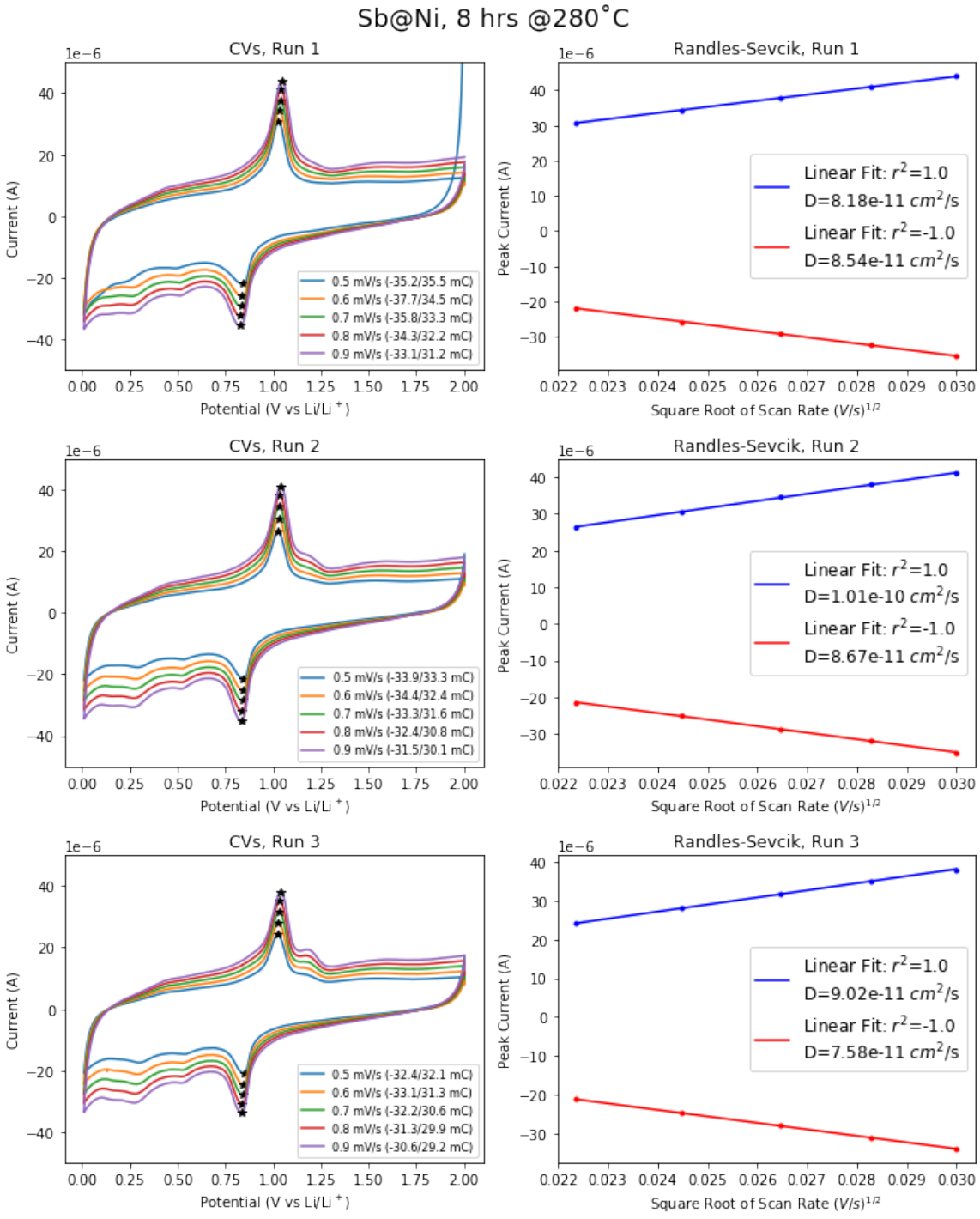

Figure S16. Variable rate CVs of the uncoated and 8 hour annealed Sb@Ni electrode with the corresponding bottleneck diffusivities calculated using the Randles-Sevcik equation.

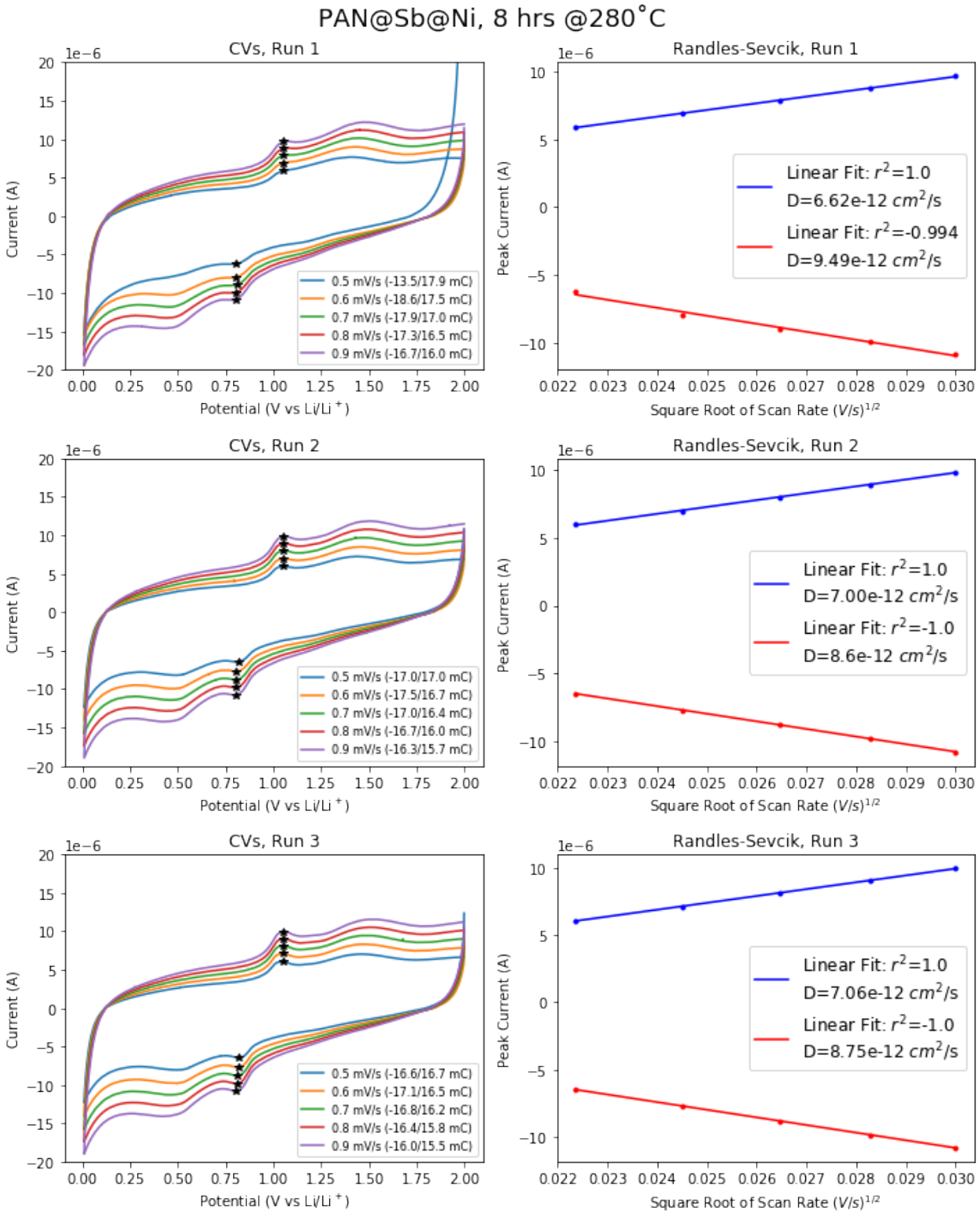

Figure S17. Variable rate CVs of the 8 hour annealed PAN@Sb@Ni electrode with the corresponding bottleneck diffusivities calculated using the Randles-Sevcik equation.

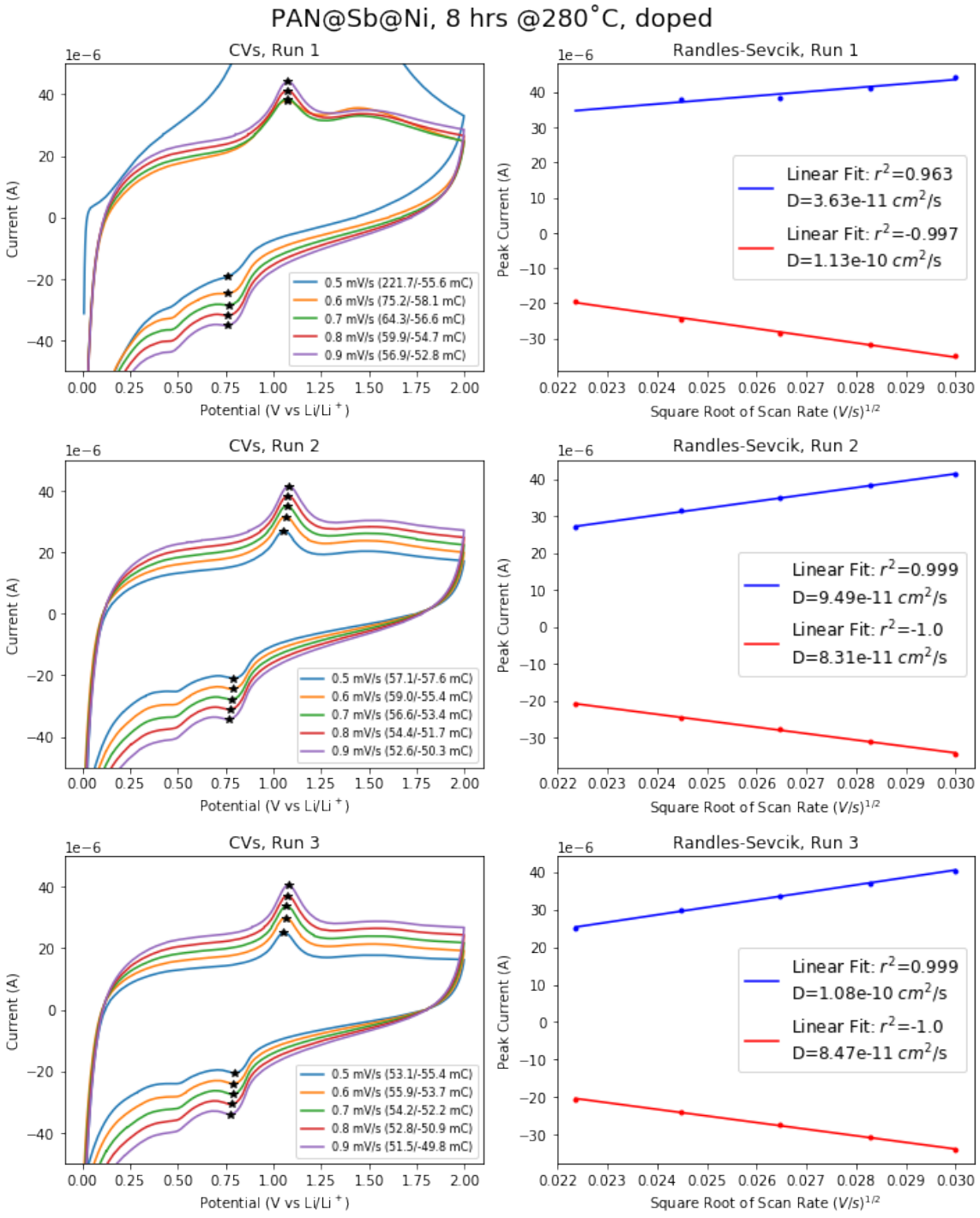

Figure S18. Variable rate CVs of the 8 hour annealed and doped (shorted) PAN@Sb@Ni electrode with the corresponding bottleneck diffusivities calculated using the Randles-Sevcik equation.

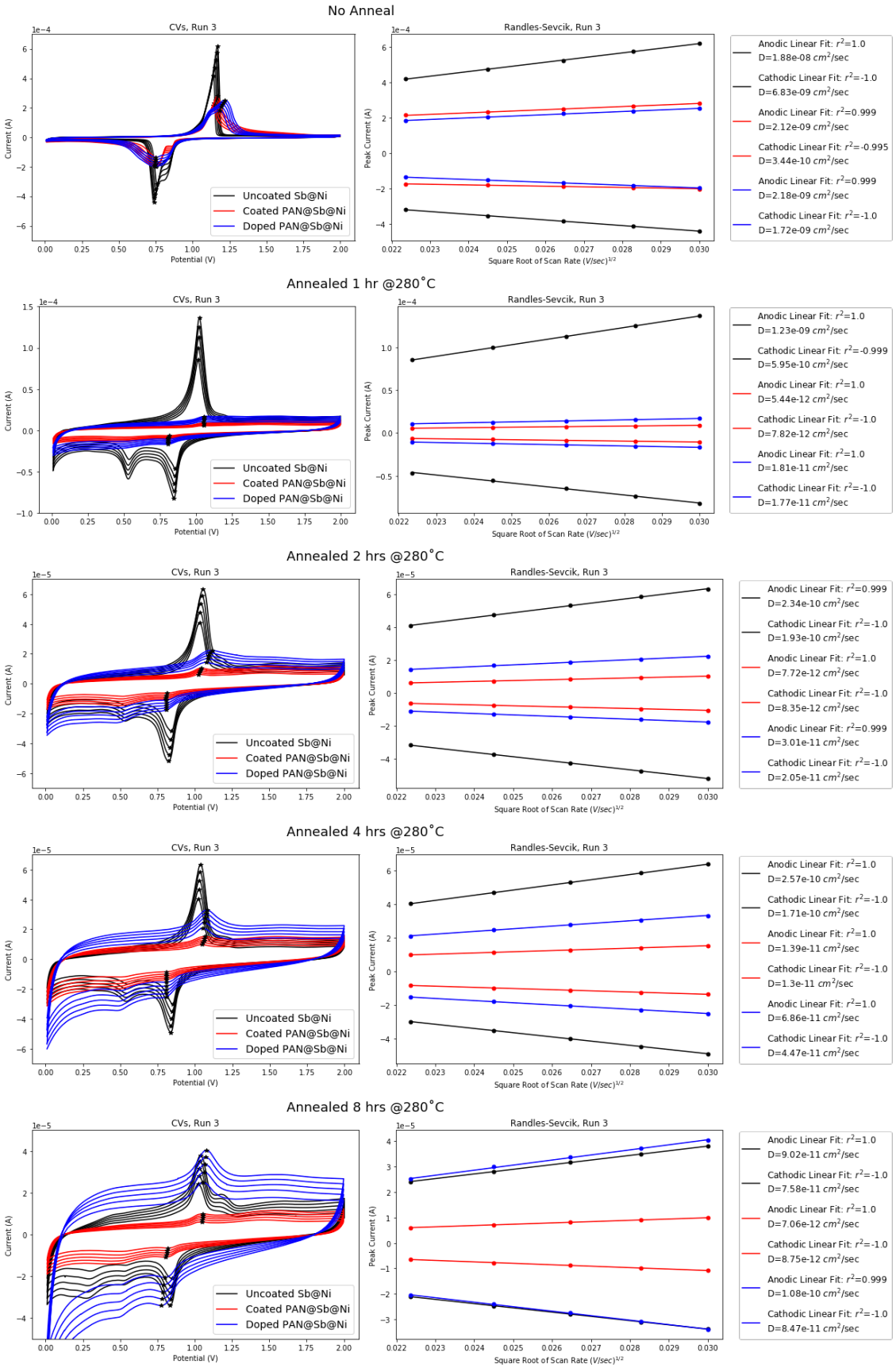

Figure S19. Variable rate CVs of all electrodes with the corresponding bottleneck diffusivities calculated using the Randles-Sevcik equation.

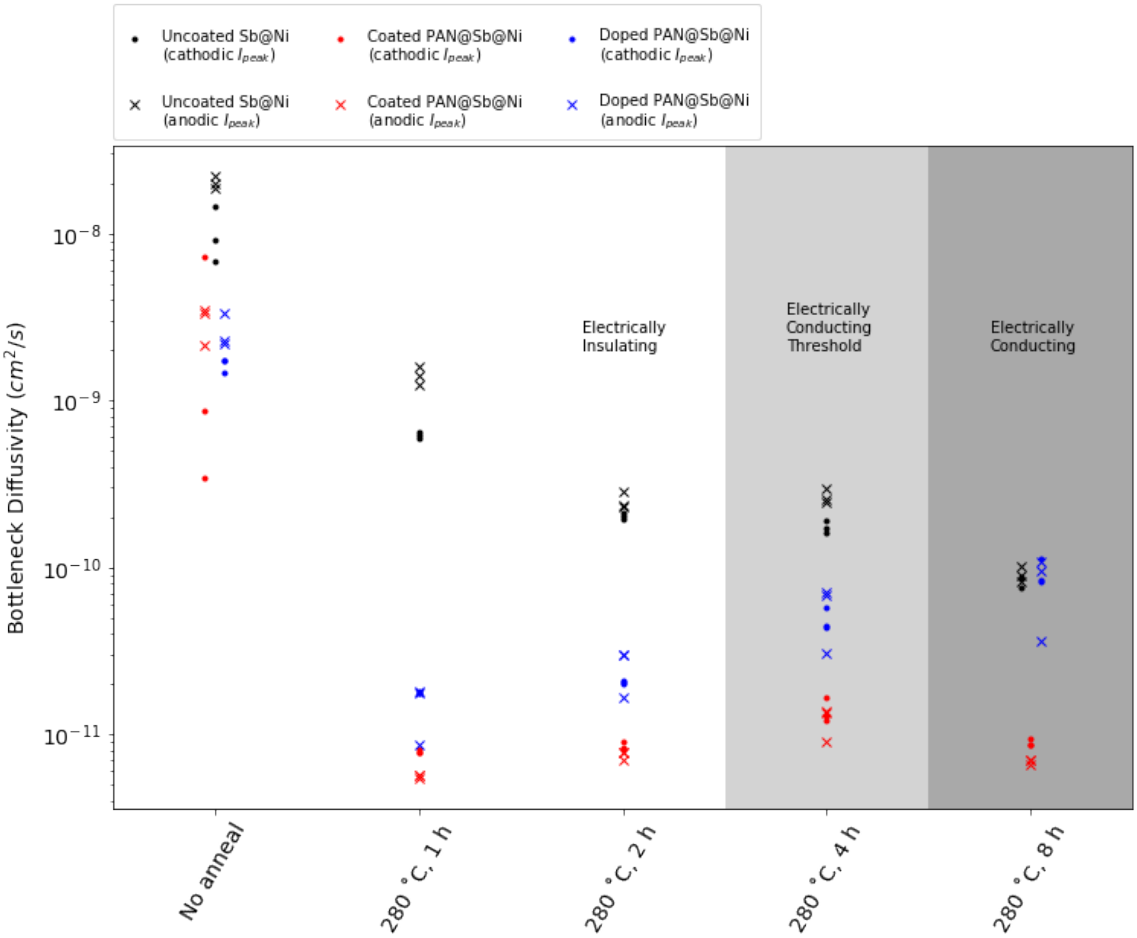

Figure S20. Bottleneck diffusivities calculated using the Randles-Sevcik equation.